Journal of Sound and Vibration 329 (2010) 2738–2750

Contents lists available at ScienceDirect

Journal of Sound and Vibration

journal homepage: www.elsevier.com/locate/jsvi

Self-tuning control systems of decentralised velocity feedback

Michele Zilletti [a,*], Stephen J. Elliott [a], Paolo Gardonio [b]

[a] Institute of Sound and Vibration Research, Highfield, Southampton SO17 1BJ, UK
[b] DIEGM, Università degli Studi di Udine, Via delle Scienze, 208, 33100 Udine, Italy

ARTICLE INFO

Article history:
Received 20 October 2009
Received in revised form
12 January 2010
Accepted 22 January 2010
Handling Editor: L.G. Tham
Available online 12 February 2010

ABSTRACT

This paper is concerned with decentralised velocity feedback for the control of vibration on a flexible structure. Previous studies have shown that a direct velocity feedback loop with a collocated force actuator produces a damping action. Multiple velocity feedback control loops thus reduce the vibration and sound radiation of structures at low frequency resonances, where the response is controlled by damping. However, if the control gains are too high, so that the response of the structure at the control point is close to zero, the feedback control loops will pin the panel at the control positions and thus no damping action is generated. Therefore, in order to maximise the active damping effect, the feedback gains have optimum values and the loops need to be properly tuned.

In this paper, a numerical investigation is performed to investigate the possibility of self-tuning the feedback control gains to maximise the power absorbed by the control loops and hence maximise the active damping. The tuning principle is first examined for a single feedback loop for different excitation signals. The tuning of multiple control loops is then considered and the implementation of a practical tuning algorithm is discussed.

1. Introduction

Active vibration control of large structures requires many actuators and sensors particularly when control is desired at audio frequencies [1,2]. Also, the control of random disturbances requires the implementation of a feedback control system, since for structural control it is normally impossible to measure in advance the spatial and time waveform of the primary excitation. There are two types of multichannel vibration feedback control systems. In the first one, all the actuators are driven by a single controller which uses the signals measured by all of the sensors. In general the number and type of actuators and sensor transducers is chosen in such a way as to measure and excite the vibration component of the structure to be controlled. Thus they do not need to be collocated and a different number of sensors and actuators may be used to selectively control different modes [1,3,4]. This arrangement is called centralised control; its design needs an accurate model of the plant responses in order to properly set the control functions and its implementation can be rather complicated. Normally the plant responses are derived from modal models which are accurate only at low frequencies where the response of the structure is controlled by a small number of modes [3]. Thus the performance and stability of such a centralised control system can be affected by changes in the operation conditions of the structure (e.g. tensioning effects, temperature variations, etc.). Also failure of one control channel can disrupt the operation of the whole control system.

* Corresponding author. Corresponding author. Tel.: +44 7892818006.
E-mail addresses: mz@isvr.soton.ac.uk (M. Zilletti), S.J.Elliott@soton.ac.uk (S.J. Elliott), paolo.gardonio@uniud.it (P. Gardonio).

0022-460X/$ - see front matter © 2010 Elsevier Ltd. All rights reserved.
doi:10.1016/j.jsv.2010.01.024

The second feedback control arrangement uses an equal number of sensors and actuator transducers, which are arranged in pairs. Each sensor–actuator pair is treated as an independent control unit so that the error signal measured by a sensor is used to drive the collocated actuator only. The advantage of this decentralised control architecture is the simplicity of the control loops, which can be simple gains for ideal force actuators and velocity sensors, whose design does not rely on a model of the plant response [2,4,5]. Since such loops are unconditionally stable [6], the failure of one control unit has no effect on the stability of the other units. Thus decentralised control systems offer a more robust but less selective approach to control, which can be based on modular control units that are evenly scattered on the structure to be controlled [5].

In this paper, a decentralised velocity feedback control system formed by pairs of collocated ideal point force and ideal velocity sensors scattered over the surface of a thin rectangular panel is considered. In a fully decentralised arrangement, global information on the response of the structure is not available at each control unit, and thus it is not possible to automatically tune the control loops in such a way that the true overall global response of the panel is minimised. This paper presents a numerical study to investigate the possibility of using the local velocity error signal of each control unit to tune it such that it approximates the global effect of minimising the spatially averaged vibration of the panel. The control principle is based on energy absorption produced by the active damping action of the feedback loops, which is particularly effective at resonance frequencies of low order modes of the panel [7–9]. Thus, in this paper the idea of self-tuning the local feedback loops such that they maximise local total power absorption is investigated. In particular it is shown that an accurate estimate of the absorbed power can be obtained, for ideal force actuation, using only the observed measured velocity. The idea of controlling vibration by maximising the total power absorbed by a control system has been investigated in the past [10–15]. However, the power has always been estimated by measuring both force and velocity in these studies. Also several of these studies have highlighted that this approach may lead to the paradox of increasing the overall response of the structure, since the controller could enhance the power injected by the primary source when the excitation frequency band is narrow, although Sharp et al. [14] emphasise the difference between this and broadband excitation. In this paper, the minimisation of total kinetic energy and maximisation of local total power absorbed by the feedback loops are compared as strategies to tune the control gain for broadband random excitation. The idea is first investigated with a single feedback loop and then with multiple feedback loops. In this way both the physics of the proposed method and its stability and performance properties are assessed. The implementation of a practical self-tuning algorithm, using the measured signal to estimate the absorbed power is then discussed.

The paper is organised into five sections. Section 2 presents the plate model problem considered in the study and briefly describes the mathematical model used to produce the simulation results. Section 3 contrasts the effects of minimising the total kinetic energy of the plate and maximising the power absorbed when only one feedback loop is used and the panel is subjected to single frequency and broadband random excitations, uniformly distributed over the surface of the plate. In Section 4, the interaction between control units is investigated by considering the implementation of two feedback loops, with local gains adapted to minimise the total kinetic energy and to maximise the local power absorbed by the feedback loops. Finally, in Section 5 the implementation of an algorithm that self-tunes the gains of multiple independent control loops to maximise the local power absorbed is discussed and its convergence behaviour is examined.

2. Mathematical model

This section outlines the model used to predict the response of the system under consideration, which, as shown in Fig. 1, is composed of a simply supported thin rectangular plate with one or multiple velocity feedback loops. The assumed geometry and physical properties of the plate are summarised in Table 1. The plate is modelled using a modal decomposition and subject to a random excitation, which is assumed to be 'rain-on-the-roof'; that is, a uniform spatial distribution of uncorrelated forces, where ω is the circular frequency, with a 'power spectral density' (PSD) constant in frequency (i.e. white noise). The overall vibration of the plate is expressed in terms of the PSD of the kinetic energy of

Table 1
Geometrical and physical parameters of the plate.

Parameter	Value
Dimensions	$l_x \times l_y = 0.414 \times 0.314$ m
Thickness	$h = 0.001$ m
Mass density	$\rho = 2700$ kg/m^3
Young's modulus	$E = 7 \times 10^{10}$ N/m^2
Poisson ratio	$\nu = 0.33$
Loss factor	$\eta = 0.01$
Control position 1	$x_1, y_1 = 0.3l_x, 0.7l_y$
Control position 2	$x_2, y_2 = 0.73l_x, 0.4l_y$

flexural vibrations, which according to reference [16] is given by

$$S_K(\omega) = \frac{1}{2}\int_0^{l_x}\int_0^{l_y} \rho h \lim_{T\to\infty} E[\dot{w}^*(x,y,\omega)\dot{w}(x,y,\omega)]\,dx\,dy = \frac{1}{2}ME[trace(\mathbf{a}(\omega)\mathbf{a}^H(\omega))] \tag{1}$$

where h, l_x, l_y are the thickness and dimensions of the panel, ρ is the density of the material of the panel and $M=\rho h l_x l_y$ is the mass of the panel. Also $\dot{w}(x,y,\omega)$ is the complex phasor of the panel transverse velocity and $E[\ ]$ is the expectation operator for a $T\to\infty$ time sample length. Finally, $\mathbf{a}$ is a column vector with the complex modal velocities produced by both the 'rain-on-the-roof' primary excitation and by S control forces. This vector can be expressed as

$$\mathbf{a} = \mathbf{a}_p + \mathbf{B}\mathbf{f}_c \tag{2}$$

where $\mathbf{a}_p$ is the vector of modal response due to the primary excitation, $\mathbf{f}_c=[f_1,\ldots f_S]^T$ is the column vector of S control forces and $\mathbf{B}$ is the coupling matrix between the control forces and the modal amplitudes. The column vector $\dot{\mathbf{w}}_c=[\dot{w}_{c1},\ldots,\dot{w}_{cS}]^T$ of the complex velocities at control positions can be expressed as follows:

$$\dot{\mathbf{w}}_c = \boldsymbol{\varphi}_c^T\mathbf{a} \tag{3}$$

where $\boldsymbol{\varphi}_c=[\varphi_{c,1},\ldots,\varphi_{c,N}]$ is the row vector with the first N natural modes of the plate at control position which have been taken from Ref. [17] for a simply supported plate. Assuming decentralised velocity feedback control loops are implemented, the control forces vector can be expressed as

$$\mathbf{f}_c = -\mathbf{G}\dot{\mathbf{w}}_c, \tag{4}$$

where $\mathbf{G}$ is a diagonal matrix with the feedback control gains.

Combining Eqs. (2)–(4) and solving with respect to $\dot{\mathbf{w}}_c$ yields:

$$\dot{\mathbf{w}}_c = (1+\boldsymbol{\varphi}_c^T\mathbf{B}\mathbf{G})^{-1}\boldsymbol{\varphi}_c\mathbf{a}_p = \mathbf{P}\mathbf{a}_p \tag{5}$$

Substituting Eq. (5) into (4) and then into (2) the vector with the complex modal velocities $\mathbf{a}$ with control then becomes:

$$\mathbf{a} = [\mathbf{I}-\mathbf{B}\mathbf{G}\mathbf{P}]\mathbf{a}_p = \mathbf{U}\mathbf{a}_p \tag{6}$$

Using the modal formulation the vector of primary modal amplitude can be written as

$$\mathbf{a}_p = \boldsymbol{\Omega}\mathbf{f}_p \tag{7}$$

where $\mathbf{f}_p$ is the modal force due to 'rain-on-the-roof' excitation, thus has the property that $E[\mathbf{f}_p\mathbf{f}_p^H]$ is equal to the identity matrix, and $\boldsymbol{\Omega}$ is the diagonal matrix of modal excitation terms, then $E[\mathbf{a}_p\mathbf{a}_p^H]=\boldsymbol{\Omega}\boldsymbol{\Omega}^*$. Substituting Eq. (6) into (1) the PSD of the kinetic energy of the plate is given by

$$S_K(\omega) = \frac{1}{2}M\,\mathrm{trace}(\mathbf{U}\boldsymbol{\Omega}\boldsymbol{\Omega}^*\mathbf{U}^H) \tag{8}$$

Considering Eq. (4), the PSD of power absorbed by the control feedback loops can be expressed as:

$$S_P(\omega) = \frac{1}{2}E\left[\mathrm{Re}\left\{\mathbf{f}_c^H\dot{\mathbf{w}}_c\right\}\right] = \frac{1}{2}E\left[\mathrm{Re}\left\{\mathrm{trace}(\dot{\mathbf{w}}_c\dot{\mathbf{w}}_c^H\mathbf{G})\right\}\right] \tag{9}$$

Thus, substituting Eq. (5) into Eq. (9), the PSD of power absorbed becomes:

$$S_P(\omega) = \tfrac{1}{2}\mathrm{trace}(\mathbf{P}\boldsymbol{\Omega}\boldsymbol{\Omega}^*\mathbf{P}^H\mathbf{G}) \tag{10}$$

3. Single feedback loop

In this section, the effects produced by only feedback control loop number 1 in Fig. 1 are investigated. The implementation of a fixed control gain g_1 for broad frequency band control is firstly considered, which either minimises the total kinetic energy of the panel or maximises the total power absorbed by the feedback loop. Secondly, the possibility of a frequency-dependent control gain is considered, which either minimises the total kinetic energy of the panel or maximises the total power absorbed at each frequency.

3.1. Fixed gain for broad frequency band control

Fig. 2 shows the PSD of the kinetic energy of the panel without control (solid line) and when the frequency independent gain of the control loop number 1 is increased from a very small value to higher values (dashed line, faint line and dotted line, respectively). For small gains, the control loop produces active damping which reduces the response of the plate up to the third resonance frequency at about 120 Hz. The faint line represents the response of the panel for the control gain that minimises the frequency averaged response of the panel. If the control gain exceeds this value, the response of the panel increases again, at other frequencies, eventually creating a new set of resonance frequencies. This is due to the fact that the control loop is pinning the panel at a control position and thus the resonance frequencies of the point-constrained simply supported panel are shifted up in frequency [18–21]. Fig. 3 shows the PSD of power absorbed by the feedback loop when the control gain g_1 is increased. The solid line provides a benchmark reference of the power absorbed for a very low value

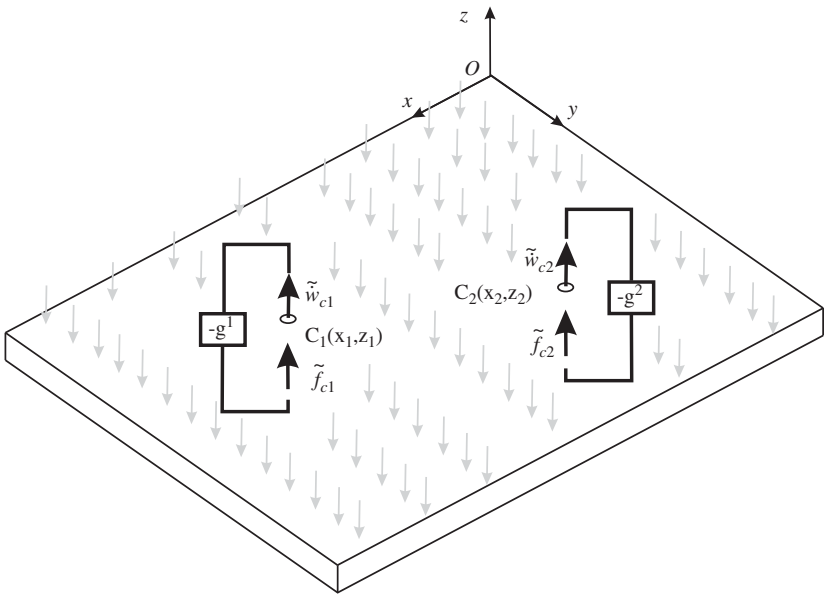

Fig. 1. Physical arrangement of multiple direct velocity feedback control loops implemented on a simply supported plate.

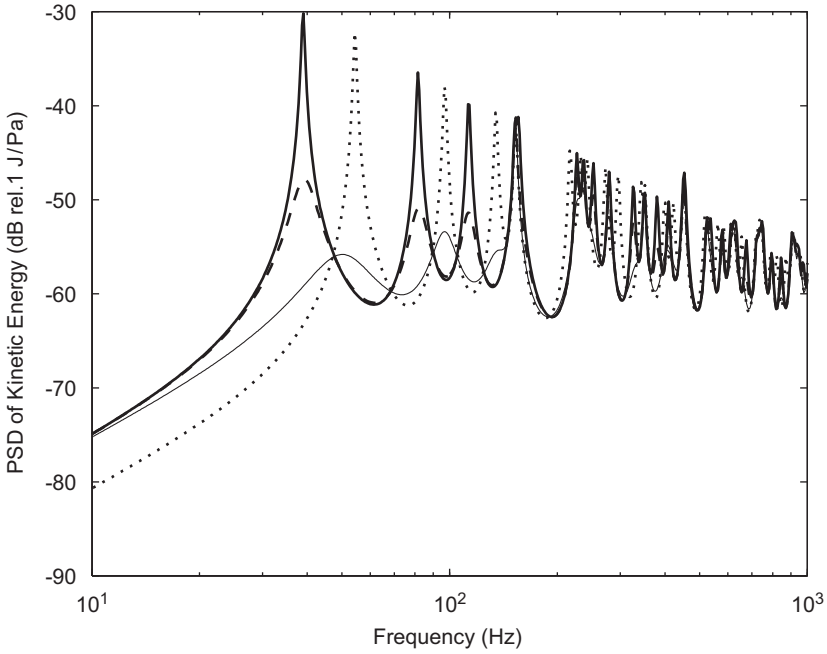

Fig. 2. PSD of the kinetic energy on the plate with a single feedback loop when g=0 (solid line), g=7 (dashed line), g=25 (faint line) and g=10^6 (dotted line).

of feedback gain (0.001). When the control gain is increased with the same values considered in Fig. 2, the spectrum of the power absorbed increases (dashed) until an optimum value of control gain (faint line) is reached. When the gain is further increased, the power absorbed decreases again as the new set of resonances emerge (dotted line). This interesting result suggests that a good level of performance can be achieved by maximising the total power absorbed by the feedback loop over a wide frequency band. This observation is confirmed by the plots in Figs. 4 and 5, which show the 1 Hz to 1 kHz frequency-integrated PSD of the total kinetic energy, normalised to the reference level without control, and the 1 Hz to 1 kHz frequency-integrated PSD of the total power absorbed, as a function of the control gain. The two plots show that as the feedback control gain g_1 is raised, the frequency integrated kinetic energy initially decreases while the frequency integrated power absorbed initially increases. The minimum of the kinetic energy and the maximum of power absorbed are achieved at about the same control gain. At higher gains, the kinetic energy increases again and the power absorbed drops off.

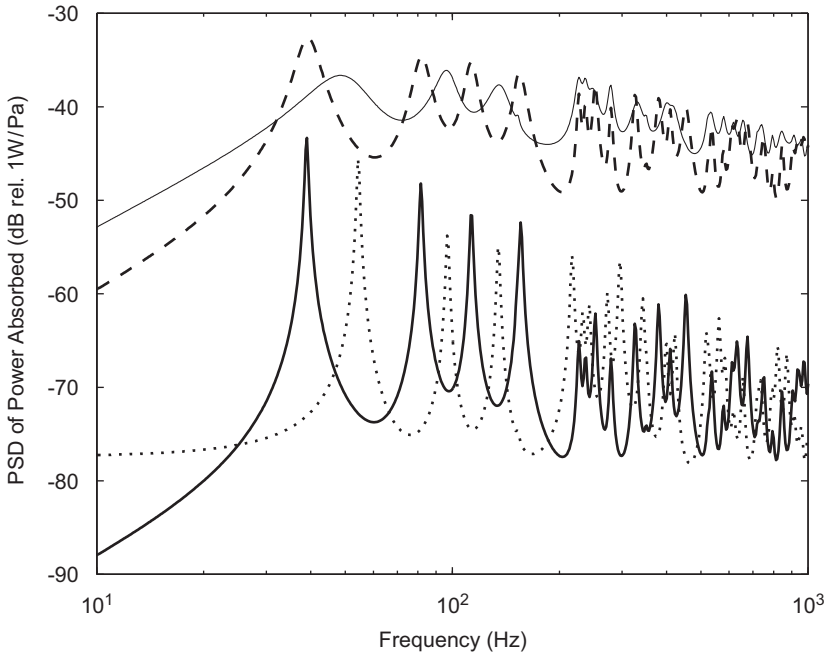

Fig. 3. PSD of the power absorbed by a single feedback loop when g=0.001 (solid line), g=7 (dashed line), g=25 (faint line) and g=10^6 (dotted line).

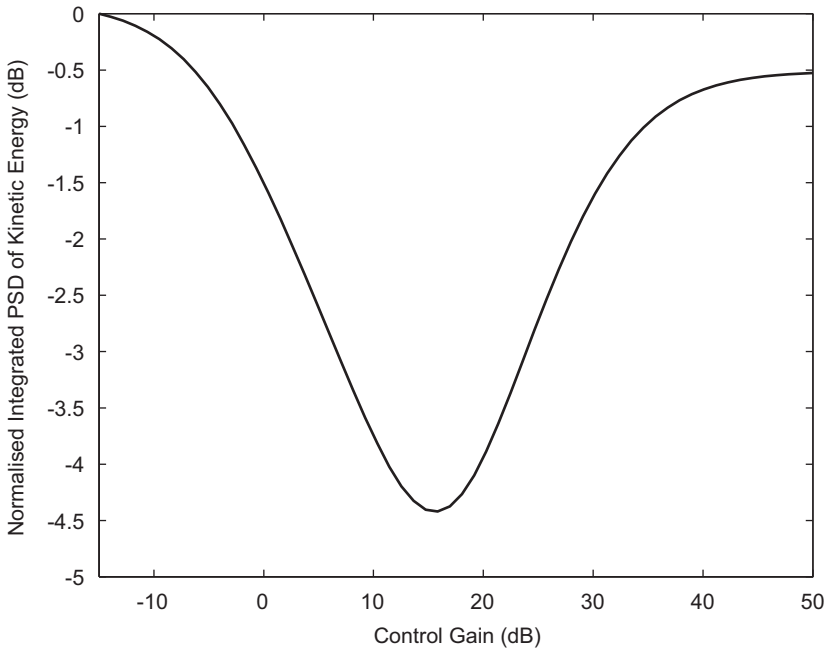

Fig. 4. Ratio of the 1 Hz–1 kHz frequency-integrated PSD of the plate total kinetic energy with and without control as function of the control gain g_1.

It has previously been noted that maximising power absorption does not minimise overall system energy for narrow band excitation [11]. The effect of excitation bandwidth on the results, shown in Figs. 4 and 5 was thus investigated. Fig. 6 shows the difference between the control gains that would produce maximum reduction of kinetic energy and maximum power absorption averaged over increasingly wider frequency bands between 1 Hz and 1 kHz. For small bandwidths the two control gains differ by about four orders of magnitude. However, when the bandwidth exceeds about 60 Hz, the difference between the two gains abruptly drops down to values between 0 and 10 dB. Fig. 7 shows a similar graph for the difference between the reductions of kinetic energy that are produced with the two control gains and shows a similar transition at 60 Hz. The 60 Hz cut-off frequency corresponds to the fundamental resonance frequency of the simply

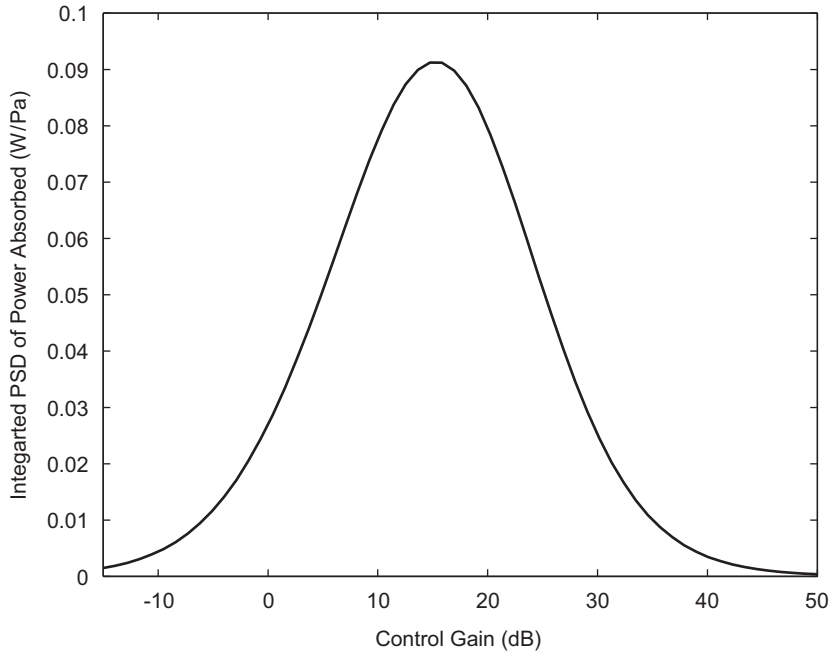

Fig. 5. 1 Hz–1 kHz frequency integrated PSD of the power absorbed by the feedback loop as function of the control gain g_1.

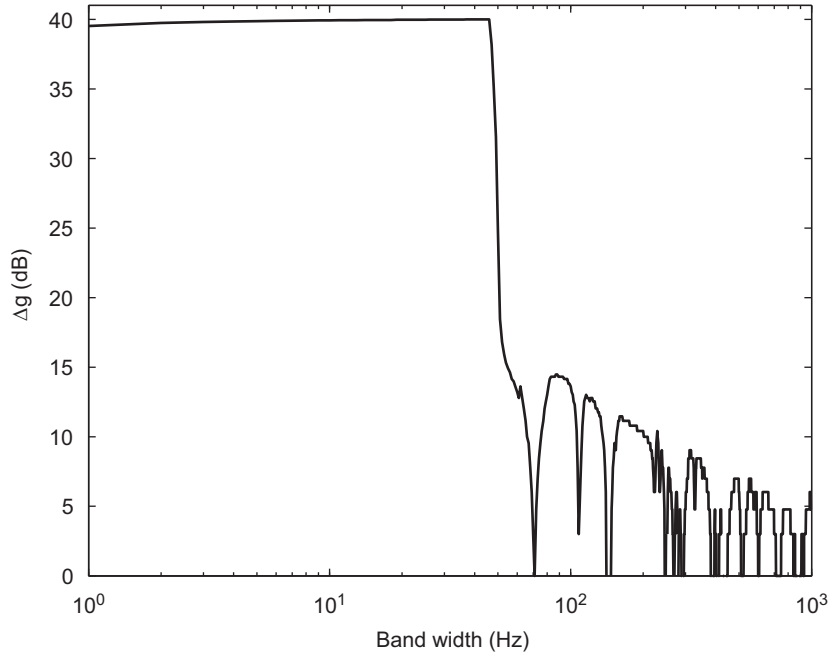

Fig. 6. Difference between the control gains minimising the kinetic energy and maximising the power absorption by the control feedback loop integrated over increasingly wider frequency bands between 1 and 1000 Hz.

supported panel with the additional pinning constraint at the control position (the first peak of the dotted spectrum is shown in Fig. 2). Maximising the total power absorbed thus minimises the kinetic energy if the frequency range over which the two quantities are integrated includes at least the fundamental resonance of the plate response when the control unit pins the panel. For smaller excitation bandwidths the kinetic energy is minimised at high feedback gains, which pin the panel, and hence produce little power absorption. The maximisation of the frequency integrated power absorbed thus only provides good reduction in kinetic energy if the frequency band on which the integration is made includes at least two of resonant frequencies of the panel.

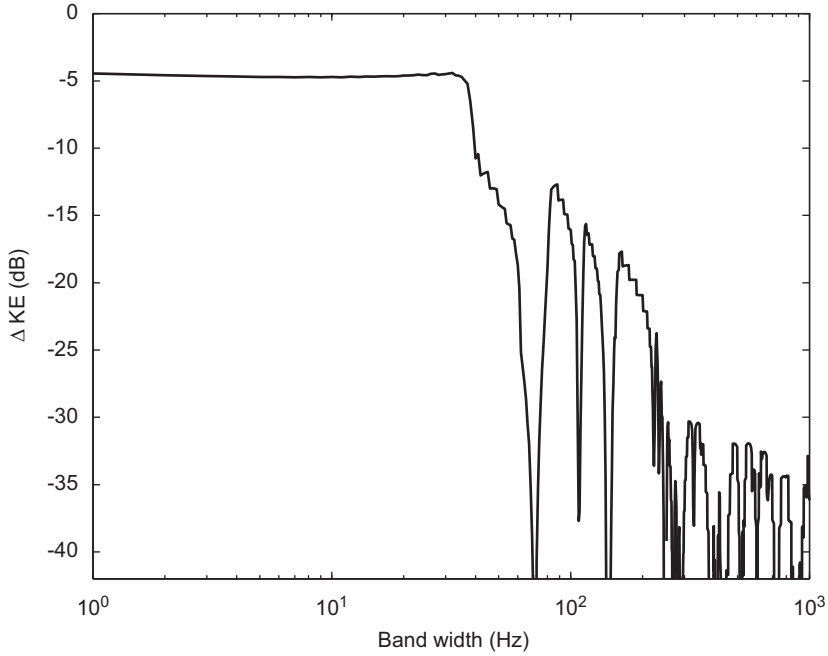

Fig. 7. Difference between the kinetic energy maximising the power absorption by the feedback loop and the minimum of kinetic energy achievable.

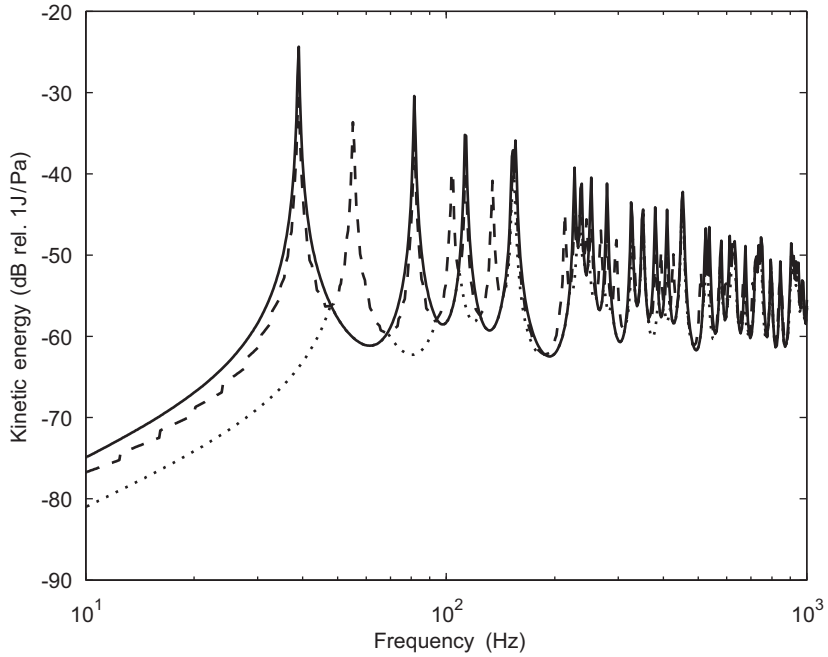

Fig. 8. Spectrum of the total kinetic energy without control (solid line), minimising the kinetic energy (dotted line) and maximising the power absorbed by the feedback loop (dashed line) implementing a frequency-dependent control gain.

3.2. *Frequency-dependent gain for narrow frequency band control*

Fig. 8 shows the spectrum of the plate kinetic energy when the plate is excited one frequency at a time and there is no control (thick line) and when the gain of control loop number 1 is set to minimise the panel kinetic energy (dotted line) or power absorbed (dashed line) independently at each frequency. The resulting frequency-dependent control gains for the two cases are shown in Fig. 9. However, it would not be possible to implement a broadband controller with frequency

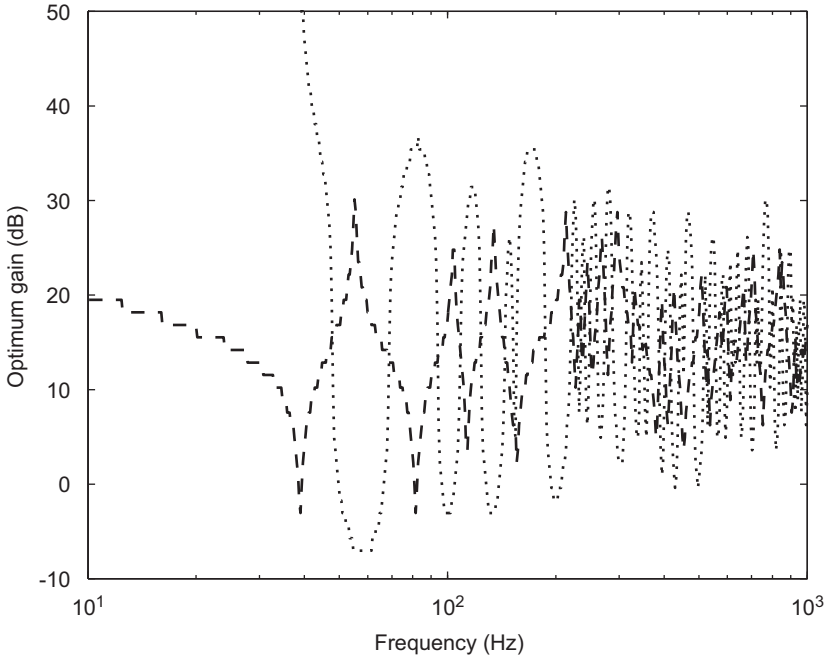

Fig. 9. Optimum gain minimising the total kinetic energy (dotted line) and maximising the total power absorbed by the feedback loop (dashed line) as function of the frequency.

responses corresponding to either of these curves, since their phase response is zero and so their impulse responses would be symmetrical in the time domain and hence non-causal. The plot in Fig. 8 indicates that, as one would expect, the best control approach is produced when the feedback gain is adjusted to minimise the kinetic energy. The other approach, where the energy absorbed by the control loop is maximised at each frequency independently, produces reductions of the kinetic energy only over small frequency bands. The resulting kinetic energy spectrum is characterised by resonance peaks and also new peaks that occur in between two resonances. The rain-on-the-roof primary excitation efficiently supplies power into the panel at its resonance frequencies, which can then be absorbed by a feedback loop tailored to maximise the power absorption and thus maximum power absorption can be induced at some frequencies by inducing new resonances. A detailed analysis of the response of the plate at the new peak at around 55 Hz, shows that the feedback loop reduces the error velocity to very low values by implementing the very large feedback gain seen in Fig. 9 at this frequency, so that a new resonant mode is generated [20]. These single frequency simulations reinforce the requirement for a significant excitation bandwidth if minimisation of power absorbed is to be used to minimise kinetic energy.

4. Multiple feedback loops

In this section, the control effects of two feedback loops are investigated when the panel is subject to broadband excitation. The positions of the two control points are given in Table 1 and they are at a distance of 0.2 m apart. The two control gains are frequency independent and are set to minimise the total kinetic energy of the panel or maximise the power absorbed by both control feedback loops. Fig. 10 shows, as a function of the two feedback gains g_1 and g_2, the 1 Hz–1 kHz integrated PSD of the total kinetic energy of the panel normalised to the reference PSD of kinetic energy without control and the 1 Hz–1 kHz integrated PSD of the total power absorbed by the two control feedback loops. The plots show that the minimum total kinetic energy and the maximum power absorbed are given when the two feedback gains are similar to the values that they would have if they were controlling the vibration of the panel independently. Moreover, the minimum total kinetic energy and the maximum total power absorbed occur for a very similar pair of control gains. This suggests that controlling the response of the panel by locally tuning each control loop to maximise its power absorbed in a wide range of frequencies can be extended to multiple feedback loops. Comparing Fig. 4 with 10(a) and Fig. 5 with 10(b), shows that using two feedback loops instead of one further reduces the total kinetic energy by about 1.5 dB and increases the total power absorbed by about 1.5 dB.

Fig. 11 show the PSD, integrated between 1 Hz and 1 kHz, of the power absorbed by the individual feedback loops as functions of the feedback gains g_1 and g_2. The two plots show that the power absorbed by each control unit is reduced when the other control unit is tuned close to its optimal value, and the control gain that maximises the power absorbed by one control unit is slightly influenced by the control gain in the other loop. The simultaneous maximisation of the local power in both control units, however, converges to the maximisation of the total absorbed power shown in Fig. 10. The

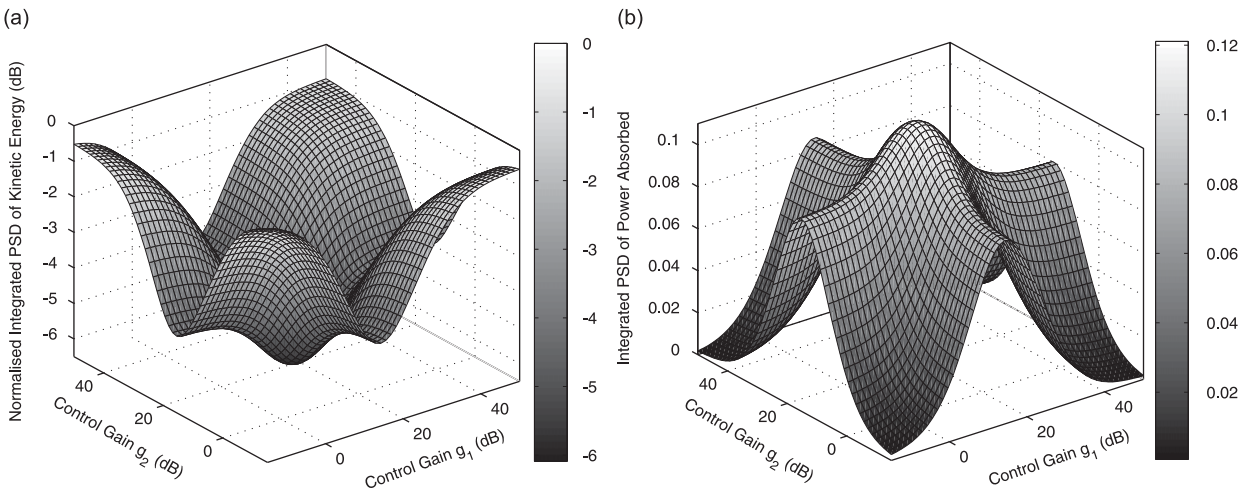

Fig. 10. 1 Hz–1 kHz frequency integrated (a) PSD of total kinetic energy and (b) PSD of total power absorbed by the two feedback loops as a function of the control gains g_1 and g_2.

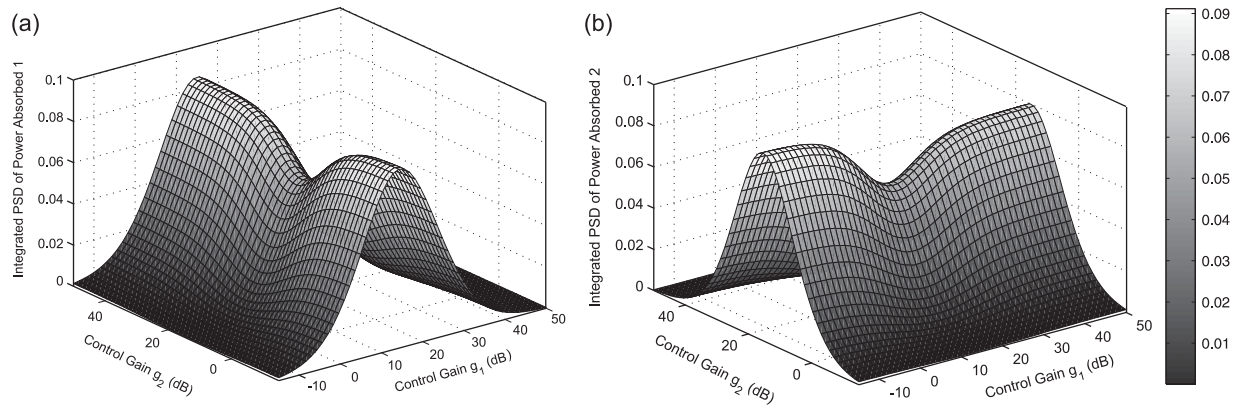

Fig. 11. 1 Hz–1 kHz PSD of power absorbed by (a) control unit number 1 and (b) number 2 as a function of the control gains g_1 and g_2.

important aspect of the curves in Fig. 11, as far as a practical adaptation algorithm is concerned, is that if one control gain is fixed, the local power absorbed by the other loop is still maximised by a single value of its control gain. It is thus possible to use gradient-based algorithms to adjust the individual control gains.

5. Self-tuning algorithm

The simulation study presented in Sections 3 and 4 has shown that assuming broadband excitation a similar control performance is achievable minimising the total kinetic energy of the plate or maximising the power absorbed by each of the feedback loops. This suggests that reductions in the overall vibration can be obtained by adapting the local feedback gains of the control units to maximise the total power absorbed by each control unit. Fig. 12 shows a potential self-tuning scheme for a local feedback loop. Since $f_{cn} = -g_n \dot{w}_{cn}$ then the power absorbed by the controller at a given frequency is given by

$$S_{pn} = \tfrac{1}{2}\,\mathrm{Re}(f_{cn}^{*}\dot{w}_{cn}) = \tfrac{1}{2} g_n |\dot{w}_{cn}|^2 \tag{11}$$

The frequency averaged power absorbed is thus proportional to the mean square velocity at the control position multiplied by the control gain. Thus an algorithm that adjusts the control gain to maximise the total power absorbed can be implemented using only the local velocity measured by the sensor, the instantaneous value of which is used as the feedback signal.

In this initial study, a simple algorithm that adjusts the control gain to maximise the total power absorbed by each loop has been investigated. The algorithm increases the control gain in each loop gradually from zero in fixed steps, then calculates the power absorbed by multiplying the value of the control gain by the mean squared velocity measured by the

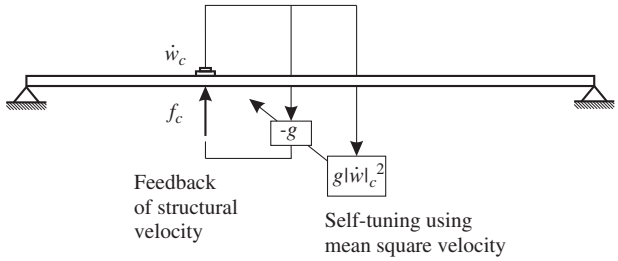

Fig. 12. Scheme of a single self-tuning velocity feedback loop.

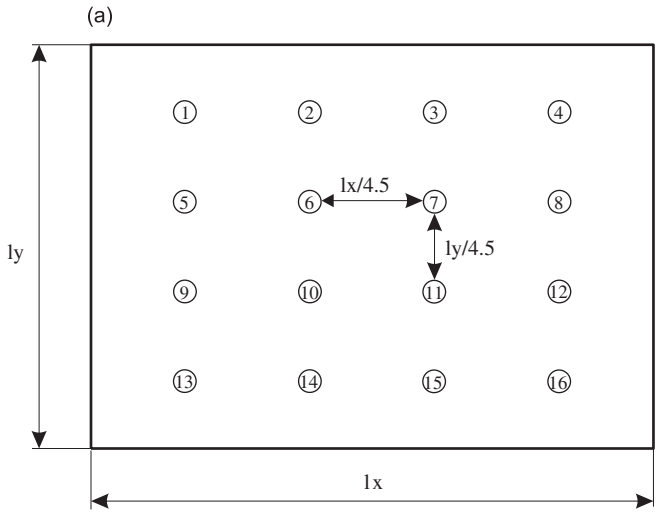

(b)

31.7	33.8	33.8	31.7
27.5	31.1	31.1	27.5
27.5	31.1	31.1	27.5
31.7	33.8	33.8	31.7

Fig. 13. (a) Scheme of a plate with the control points disposition and (b) values of control gain maximising the power absorbed of each control feedback loop.

local sensor. The algorithm at the nth iteration can be written as

$$g(n+1) = g(n) + \alpha(n)\{sgn[\Delta P(n)]sgn[\Delta g(n)]\} \tag{12}$$

where sgn[ ] signifies the sign of the parameter in brackets, ΔP and Δg are the differences in power absorbed and control gain between two consecutive iterations with all the other control gains fixed. The parameter $\alpha(n)$ is the step by which the gain is increased at the nth iteration. When the power absorbed starts to decrease, the algorithm reduces the control gain by half a step and so $\alpha(n)$ is given by

$$\alpha(n+1) = \alpha(n) - \frac{\alpha(n)}{4}\{1 - \mathrm{sgn}[\Delta P(n)]\} \tag{13}$$

where the initial value of α for $n=0$ must be specified. The error in the estimation of g after n iterations is $\pm 2\alpha(n)$ and since $\alpha(n)$ decreases in size with n, the algorithm converges to the optimum. If the conditions on the plate change, it is assumed that this can be detected and the value of $\alpha(n)$ re-initialised so that the algorithm can adapt the gain to its new optimum value. When multiple feedback loops are tuned simultaneously, the power absorbed by one feedback loop is influenced by all the others, as shown in Section 4. Therefore, the individual power absorbed by the ith control loop must be re-estimated, keeping all the other gains constant, before the ith control gain is varied. A limitation of this tuning algorithm is thus that global synchronization is required to ensure sequential tuning, even though each control loop is still tuned using only the signal of the collocated sensor in decentralised manner. It is not clear whether other control algorithms, which allow simultaneous adaptation of each control loop, could be used and thus avoid the need for global synchronisation of the tuning.

5.1. 16 Self-tuning feedback loops

In this section, the effects of implementing 16 self-tuning feedback loops on the panel are investigated. Fig. 13 shows the positions of the control points on the panel. Fig. 13(b) shows the value of the control gains of each feedback loop after the self-tuning algorithm given in Eq. (12) has been used to tune all the feedback loops sequentially to maximise their

power absorbed. The way this is achieved is that the gain on the first control loop is adjusted using Eq. (12), and then each of the other loops are adjusted, after which this sequence is repeated until the gains have converged. The gain distribution is symmetric, as expected, but within the range 27.5–33.8. Fig. 14 shows the PSD of the panel's kinetic energy without control (solid line), when the self-tuning algorithm is used on each feedback loop (dashed line) and when the total kinetic energy is minimised off line using the same value of gain for each feedback loop (dotted line). Although the kinetic energy PSD is only shown up to an excitation frequency of 1 kHz in Fig. 14, the simulations were performed with an excitation bandwidth up to 10 kHz. This is to include the new resonance frequencies that would be created with high gains in each of these 16 feedback loops, which may interfere with the adaptation process. The plot demonstrates that the self-tuning algorithm provides an overall reduction very close to the minimum that would be achieved if the total kinetic energy is minimised using equal control gains, yet only uses information local to the control loops.

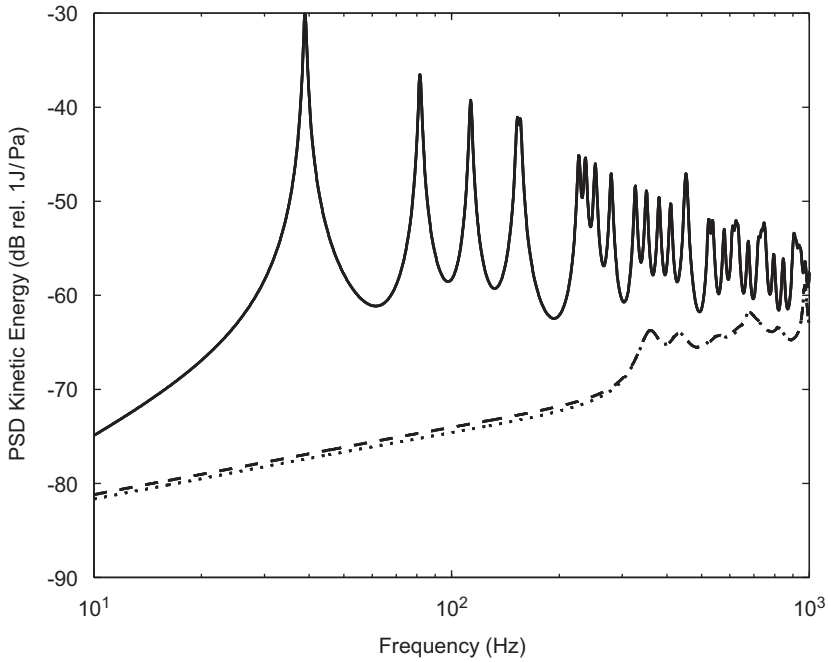

Fig. 14. PSD of the total kinetic energy when g=0 (solid line), the self-tuning algorithm is implemented (dashed line) and g_{1-16}=32.7 (dotted line).

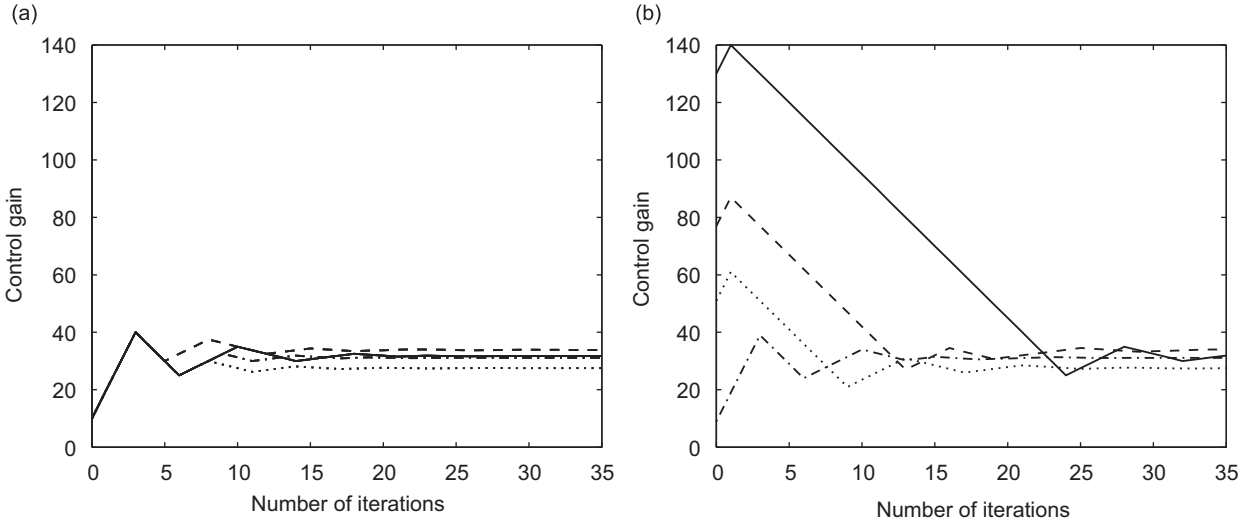

Fig. 15. Convergence of control gains g_1 (solid line), g_2 (dashed line), g_5 (dotted line) and g_6 (dash-dot line) (a) starting from 0 and (b) random values.

(a)

31.4	35.1	35.1	32.0
27.1	✗	31.5	25.9
28.1	✗	31.5	✗
31.5	34.5	34.6	29.7

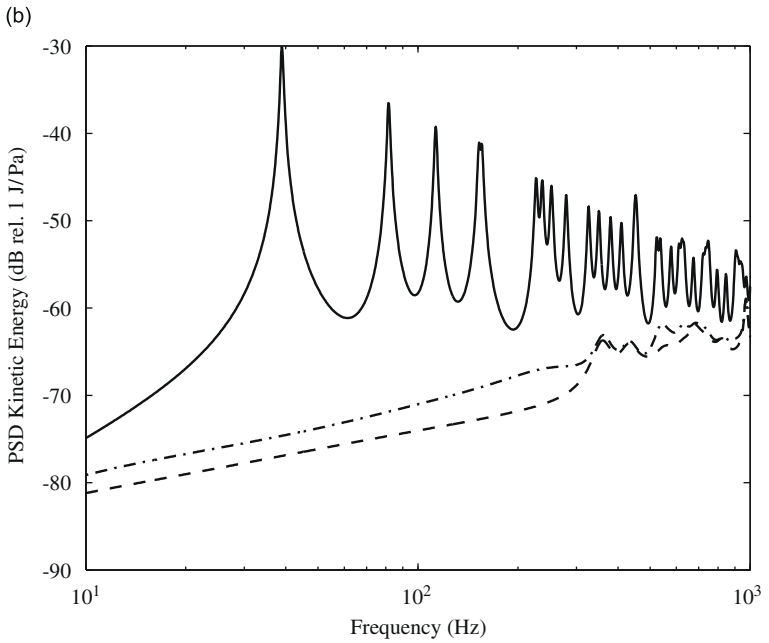

Fig. 16. (a) Control gains after convergence when the control unit 6, 10, and 12 fail after 5 iterations and (b) PSD of the total kinetic energy of the panel without control (solid line), using 16 self-tuning control loops (dashed line) and after failure of three control units (dot-dashed line).

5.2. Convergence of the algorithm

Fig. 15 shows the convergence of the algorithm for the control gains g_1, g_2, g_5 and g_6 (a) when their initial value is set on 0 and (b) when they are set to random values tuning all the feedback loops sequentially. In the simulations the initial value of alpha is set on 10 and the error on the estimation of g which is twice the minimum alpha is ± 0.02. Fig. 15 illustrates that the algorithm reliably converges to the correct optimum values, within these limits, whatever the initial conditions. Fig. 16 shows the simulation results when the control unit 6, 10 and 12 fail after 5 iterations and the corresponding values of g are then set to zero. Comparing Fig. 13(b) and Fig. 16(a), the converged values of the control gains vary slightly from those above when the three units fail, but still maximise the power absorbed in the remaining units. Fig. 16(b) shows the PSD of the kinetic energy of the panel without control (solid line), using 16 self-tuning control units (dashed line) and after the convergence of the algorithm when the three control units fail (dot-dashed line). The plot shows that after the failure, the remaining feedback gains have been slightly adjusted, but a good reduction of vibration is still achieved over this frequency range.

6. Conclusions

This paper has proposed a simple approach to automatically tune the frequency independent gains of decentralised velocity feedback control loops mounted on a plate structure, using only the measured error sensor signal. The simulation study has shown that, in the case of broadband excitation, similar control gains are required to minimise the total kinetic energy of the plate and to maximise the local total power absorbed by each of the control feedback loops. This means that overall vibration reduction of the plate structure can be obtained by adapting the local feedback gains of the control units in such a way as they maximise their own power absorption. The importance of this finding becomes even more pronounced when it is observed that the power absorbed by the local feedback loop with a collocated point force source and velocity sensor is given by the product of the mean squared value of the measured velocity and the control gain, so that the cost function to be minimised can be directly derived from the local velocity signal. Simulation results have also shown that the proposed self-tuning algorithm is robust to changes in the initial values of the control gains and to failure of one or more control loops. An important assumption in this study has been that a perfect force actuator can be used. In practice this means that the actuator must have a structure to react off, which could be achieved using a reactive electrodynamic actuator for example. The velocity signal could conveniently be obtained by integrating the output of an accelerometer.

Acknowledgements

The work done by Michele Zilletti for this paper was supported by the “Smart Structures”, ITN Marie Curie programme which is funded by the European Commission.

References

[1] C.R. Fuller, S.J. Elliott, P.A. Nelson, *Active Control of Vibration*, Academic Press, London, 1996.
[2] F.J. Fahy, P. Gardonio, *Sound and Structural Vibration*, Elsevier, London, 2007.
[3] R.L. Clark, W.R. Saunders, G.P. Gibbs, *Adaptive Structures*, 1st ed, John Wiley & Sons, New York, 1998.
[4] A. Preumont, *Vibration Control of Active Structures*, 2nd ed, Kluwer Academic Publishers Group, 2002.
[5] S.J. Elliott, Global vibration control through local feedback, in: D. Wagg, I. Bond, P. Weaver, M. Friswell (Eds.), *Adaptive Structures: Engineering Applications*, John Wiley & Sons Ltd., 2007, pp. 59–87.
[6] M.J. Balas, Direct velocity feedback control of large space structures, *Journal of Guidance and Control* 2 (1979) 252–253.
[7] S.J. Elliott, P. Gardonio, T.C. Sors, M.J. Brennan, Active vibro-acoustic control with multiple feedback loops, *Journal of the Acoustical Society of America* 111 (2) (2002) 908–915.
[8] P. Gardonio, S.J. Elliott, Smart panels for active structural acoustic control, *Smart Materials and Structures* 13 (2004) 1314–1336.
[9] W.P. Engles, S.J. Elliott, Optimal centralised and decentralised velocity feedback control on a beam, *Smart Materials and Structures* 17 (2) (2008).
[10] W. Redman-White, P.A. Nelson, A.R.D. Curtis, Experiments on the active control of flexural wave power flow, *Journal of Sound and Vibration* 112 (1) (1987) 187–1910.
[11] P. Bardou, S.J. Gardonio, S. Elliott, J. Pinnington, Active power minimization and power absorption in a plate with force and moment excitation, *Journal of Sound and Vibration* 208 (3) (1997) 111–151.
[12] N. Hirami, Optimal energy absorption as an active noise and vibration control strategy, *Journal of Sound and Vibration* 200 (3) (1997) 243–259.
[13] N. Hirami, An active maximum power absorber for the reduction of noise and vibration, *Journal of Sound and Vibration* 200 (3) (1997) 261–279.
[14] S.J. Sharp, P.A. Nelson, P.A. Koopmann, A theoretical investigation of optimal power absorption as a noise control technique, *Journal of Sound and Vibration* 251 (5) (1997) 927–935.
[15] P.J. Remington, R.D. Curtis, R.B. Coleman, J.S. Knight, Reduction of turbulent boundary layer induced interior noise through active impedance control, *Journal of the Acoustical Society of America* 123 (3) (2008) 1427–1438.
[16] J.R. Rohlfing, Gardonio, Comparison of active structural acoustic control on homogeneous and composite sandwich panels under deterministic and stochastic excitation, *ISVR Technical Memorandum* no. 984, 2009.
[17] P. Gardonio, M.J. Brennan, Mobility and impedance methods in structural dynamics, in: F.J. Fahy, J. Walker (Eds.), *Advanced Applications in Acoustics, Noise and Vibration*, E & FN Spon, London, 2004, pp. 387–388.
[18] D.K. Miu, Physical interpretation of transfer function zeros for simple control systems with mechanical flexibilities, *Transactions of the ASME, Journal of Dynamic System, Measurement, and Control* 113 (1991) 419–424.
[19] T. Williams, Constrained modes in control theory: transmission zeros of uniform beams, *Journal of Sound and Vibration* 156 (1) (1992) 177–179.
[20] P. Gardonio, S.J. Elliott, Modal response of a beam with a sensor–actuator pair for the implementation of velocity feedback control, *Journal of Sound and Vibration* 284 (2005) 1–22.
[21] Preumont, de Marneffe, Krenk, Transmission zeros in structural control with collocated multi-input/multi-output pairs by AIAA, *Journal of Guidance Control, and Dynamics* 31 (2) (2008).